

# Mind the Gap! A Study on the Transferability of Virtual vs Physical-world Testing of Autonomous Driving Systems

Andrea Stocco, *Member, IEEE Computer Society*, Brian Pulfer and Paolo Tonella, *Member, IEEE Computer Society*

**Abstract**—Safe deployment of self-driving cars (SDC) necessitates thorough simulated and in-field testing. Most testing techniques consider virtualized SDCs within a simulation environment, whereas less effort has been directed towards assessing whether such techniques transfer to and are effective with a physical real-world vehicle.

In this paper, we leverage the Donkey Car open-source framework to empirically compare testing of SDCs when deployed on a physical small-scale vehicle vs its virtual simulated counterpart. In our empirical study, we investigate transferability of behavior and failure exposure between virtual and real-world environments on a vast set of corrupted and adversarial settings. While a large number of testing results do transfer between virtual and physical environments, we also identified critical shortcomings that contribute to the reality gap between the virtual and physical world, threatening the potential of existing testing solutions when applied to physical SDCs.

**Index Terms**—AI Testing, Self-Driving Cars, Simulated Testing, Real-World Testing, Deep Neural Networks, Autonomous Vehicles.



## 1 INTRODUCTION

Self-driving cars (SDCs, hereafter) are automotive cyber-physical systems capable of sensing the environment and moving safely with little to no human driver input. Modern SDCs are realized with electric vehicles (EV) equipped with sensors such as cameras, LIDAR and GPS. Sensory data are processed by deep neural networks (DNNs) to generate predictions used to make driving decisions. The consolidated industrial practice is to first collect real-world driving data that are recreated on high-fidelity and physically accurate simulators for large-scale testing. Then, the DNNs performance is assessed in real-world environments and vehicles, typically on private test tracks [1], [2], [3], [4].

Existing DNN testing techniques from the software engineering literature, e.g., DeepXplore [5], DeepTest [6], and DeepRoad [7], test the driving decision-making DNNs through *model-level testing* (sometimes referred to as *offline testing* [8], [9]), which means that the DNN (the model) is tested in isolation and on individual inputs, rather than considering the flow of inputs experienced in a simulation or in the real world. This does not take into account that each prediction (and subsequent driving decision) influences future events, which in turn influence future predictions and driving decisions. Thus, failures found by model-level testing (i.e., simple individual prediction errors) are hardly representative of real failures occurring when the DNN is embedded onto a vehicle [8].

Specific, system-level, testing solutions for SDCs have been proposed [6], [7], [10], [11], [12], [13], [14], [15], in which the dominant approach for the empirical evaluation relies on the use of simulators, which does not guarantee that the observed failures, or lack thereof, correlate with those observable during on-road testing. Recent works have confirmed the need for real-world testing for robotic systems, as simulation platforms are often decoupled from the real world complexities [16], [17]. As such, it would be important to ground the progress done in autonomous vehicle testing on both real-world environments and physical self-driving platforms. Unfortunately, full-scale SDC testing presents severe time, space and cost constraints [18], [19].

To mitigate these limitations, small-scale vehicles have emerged as an interesting alternative. Frameworks such as Donkey Car [20] or AWS DeepRacer [21] are adopted at the early stages of testing autonomous driving algorithms as they retain relevant photorealistic conditions of the driving environment which are experienced also by full-scale cars [18]. Moreover, these platforms are increasingly used by researchers who want to experiment their machine learning algorithms on real vehicles [22], [23], [24], [25].

In this paper, we seize the opportunity of using small-scale vehicles to perform a comparative study between *simulated and real-world testing of SDCs* and quantify the reality gap between testing environments. In our study, we leverage the Donkey Car platform [20], which allows developers to deploy a DNN that performs autonomous driving both on a 1:16 scale EV in a real test track as well as its virtualized counterpart.

We evaluate and test three state-of-the-art lane-keeping DNN models, i.e., Nvidia’s DAVE-2 [26], Chauffeur [27], and Epoch [28], through *in-vitro* digital-controlled simulations and *in-vivo* observations of deployed models in a

- *Andrea Stocco and Paolo Tonella are with the Università della Svizzera italiana, Switzerland.*
- *Brian Pulfer is with the University of Geneva, Switzerland. The work has been carried out while at the Università della Svizzera italiana, Switzerland.*

real-world physical environment. We compared the testing results obtained in the virtual vs the real world, in terms of quality of driving and exposed failures. First, we assessed the transferability of driving behavior, using common driving quality metrics [10]. We found that steering angle predictions are statistically indistinguishable, whereas the SDCs’ trajectories and the DNN models’ uncertainties have non-negligible differences across the virtual and real-world environment. Second, we studied failure exposure on 642 simulations under image corruptions and adversarial examples, finding that failures due to corruptions are more frequent in the physical environment and have higher severity, whereas SDCs in the real world are more robust to adversarial attacks. Our analysis also revealed that models’ uncertainty data from the virtual simulations allow halving the number of time- and cost-intensive physical tests.

The main contribution of this paper is the first empirical work that compares simulated vs real-world testing of SDCs at the system level, using a real-world EV. Our empirical study evaluates the transferability of driving behavior and failure exposure across environments. A practical takeaway message of our study is the usage of predictive uncertainty as an effective means for reducing the cost of real-world physical testing.

## 2 BACKGROUND

### 2.1 Model-level vs System-level Testing

DNN models are typically tested by measuring either accuracy, mean squared error (MSE), mean absolute error (MAE), or other prediction metrics, on an unseen *test set* of observations that were not used to train the model. We refer to this modality of testing as *model-level testing* [29], because the model is tested as a standalone component, evaluating the predictions it makes on stationary datasets. This level of testing is comparable to unit testing for traditional software and is used by test engineers to reveal inadequately trained models [30]. For DNN-based autonomous vehicles, model-level testing is ineffective in production. Studies [8], [9] have shown that MSE is not a good estimator of the DNN’s performance in the field, because it is not possible to identify and anticipate the causal chain from the individual, possibly small, prediction errors to failures. For this reason, in our work, we focus on *system-level testing*, in which the DNN is embedded within a SDC to test the decision-making process, i.e., the effects that the predictions made by the DNN have on the behavior of the whole system. Thus, *system failures* manifest as deviations from the expected system’s behavior. For instance, safety requirements are violated when the vehicle drives off-road or causes harm to other vehicles, to the environment, or to people [11].

### 2.2 Virtual vs Physical Testing Scenario

System-level testing is often performed extensively within a simulation platform (e.g., CARLA [31] or DeepDrive [32]), referred to as *software-in-the-loop* (SIL), in which it is possible to measure, analyze, characterize, and reproduce driving failures safely. However, most simulators lack photo-realism and cannot reproduce real-world driving scenes with high fidelity and the question of whether the testing results would generalize to the real world remains open [17].

Thus, on-road system-level testing with a real physical vehicle—referred to as *hardware-in-the-loop* (HIL)—remains quite important, despite being very expensive in terms of resources and time. For safety and logistic reasons, after simulated testing, SDC manufacturers perform on-road system-level testing on *closed-loop private tracks* [3]. Only after the SDC is adequately tested within simulated and closed-loop tracks, the SDC is tested on *public roads* [1], [3].

In our work, we study system-level testing of SDC models that perform *behavioral cloning*, i.e., the autopilot learns the *lane keeping* functionality from a dataset of driving scenes collected from a human driver. Our focus is on the comparison between virtual and physical closed-loop track testing. In the rest of the paper, we shall use the terms virtual/digital/simulated, as well as the terms physical/real-world, interchangeably).

## 3 TESTBED

### 3.1 Donkey Car

We use the Donkey Car™ open-source framework [20] as the main testbed for our study. The framework includes open hardware to build 1:16 scale radio-controlled (RC) cars with self-driving capabilities, a Python framework that supports training and testing of SDCs that perform lane-keeping using supervised learning, and a simulator in which the real-world DonkeyCar is modeled with high fidelity, which allows to train and test the SDC without hardware.

Among the RC platforms available on the market, only Donkey Car fulfills our requirements for transferability studies between simulated and real-world testing of lane-keeping SDCs. For instance, DeepPiCar [33] and JetRacer [34] lack a simulator, while the AWS DeepRacer [21] would restrict us to the usage of the AWS technology and is designed mostly to study RL-based autonomous vehicles, which is not the focus of this paper. Moreover, the Donkey Car framework has already been used to experiment with autonomous driving software deployed on a real vehicle [18], [22], [23], [24] and has an affordable cost.

### 3.2 Framework and Simulation Platform

The Donkey Car framework provides Python scripts to drive the car manually, train DNN models, and deploy them. The typical usage of the framework is as follows. First, training data are collected by manually driving the Donkey Car through a web interface using a joystick or a virtual trackpad (we used a PS4® controller). Each image is associated with the throttle and steering angle values that were observed when the frame was recorded. Second, the framework supports the training of DNN models written in Keras/Tensorflow [35]. Finally, the newly trained model is evaluated on its capability of controlling the vehicle. Note that these steps can be carried out both in the real world and in the DonkeyCar simulator, developed on top of Unity [36].

## 4 METRICS

Our study requires collecting comparable driving profiles both in virtual and physical environments. We assess and compare the quality of driving by analyzing the distributions of three metrics, namely *steering angle*, *lateral deviation*,

and *predictive uncertainty*. The first two metrics are proposed by Jahangirova et al. [10] as effective metrics to evaluate the lane-keeping capability of SDC models. The last metric is used in the self-driving car domain to account for the DNN model’s confidence [37].

#### 4.1 Steering Angle

The main prediction computed by the DNN of the SDC consists of real numbers between  $[-1, \dots, +1]$ , where positive values indicate turning right, negative values indicate turning left, near-zero values indicate going straight.

In our *virtual* platform, a steering angle of +1 corresponds to  $25^\circ$ , whereas a steering angle of -1 corresponds to  $-25^\circ$ . In the *physical* Donkey Car, steering angles are converted into the vehicle’s pulse lengths by an actuator called pulse-width modulation (PWM) servo motor. Prior to running experiments, we calibrated the PWM servo motor of the Donkey Car to match such angles. For our physical car, we found the values  $\text{STEERING\_LEFT\_PWM} = 480$  and  $\text{STEERING\_RIGHT\_PWM} = 280$  to correspond to  $\pm 25^\circ$ .

#### 4.2 Lateral Deviation (XTE)

In our setup, the car follows the middle line on a two-lane road (as if it were a single-lane, one-way road) and moves only forward. Thus, the lateral position is regarded as the key telemetry value to assess the lane-keeping capability of SDC models, as shown by a recent study [10].

In our *virtual* platform, we manually placed an ordered sequence of 22 waypoints onto the simulated track along the center of the road, to allow tracking the XTE of the vehicle during motion. Then, the simulator measures the lateral position [10], or cross-track error (XTE), as the distance between the car’s cruising position and the segment between the two closest consecutive waypoints [38].

In the *physical* platform, XTE is not available from the physical vehicle as only camera images, steering angle, and throttle values are collected by the Donkey Car. Thus, we implemented a *visual odometry* solution to estimate the lateral position by processing the onboard camera images [39] during the ego-motion of the physical SDC.

Our visual odometry solution uses neural style transfer and convolutional neural networks to build a telemetry data predictor that can operate on real-world driving images. We leverage the simulator to collect thousands of driving images paired with perfect telemetry (XTE) labels. However, an XTE predictor trained on such a dataset work on virtual, not real-world images. Thus, we train a generative adversarial network called CycleGAN [40] to create images that “look like” they were drawn from the real-world distribution. Then, we train a telemetry predictor that uses such generated data, labeled with the original labels from the simulator. The use of CycleGAN [40] frees us from the constraint of collecting paired sets of images across environments, with the only requirement that they represent analogous driving images.

Our XTE predictor is a deep neural network that tackles a regression task, i.e., predicting a continuous value (e.g., the XTE) from a driving image. The DNN architecture is based on the pioneering work by Borjarski et al. [26] on processing imagery data with convolutional neural networks.

The network is composed of one normalization layer, five convolutional layers, and two fully connected layers. The first three convolutional layers use a  $2 \times 2$  stride and  $5 \times 5$  kernel; the last two convolutional layers are non-strided with a  $3 \times 3$  kernel.

We train our telemetry predictor on *pseudo-real images* produced by CycleGAN, labeled with telemetry values obtained from the simulator for the simulated images (i.e., the CycleGAN’s input). On the other hand, at prediction time the input to the predictor is a real-world image. Since the XTE predictor is quite important for our empirical study, we evaluate its accuracy with a dedicated RQ (Section 5).

In both simulated and real-world environments, we use XTE to flag the car as off-road if the car deviates by more than half of the track’s width (i.e.,  $|XTE| > 2.22$ , as  $-2$  and  $+2$  mark the lanes’ borders; 0 represents the middle of the lane, and  $-1, +1$  are in-between).

#### 4.3 Predictive Uncertainty

We measure predictive uncertainty with the variance of dropout-based DNNs’ predictions, estimated using the Monte Carlo (MC) method, or MC-Dropout [41]. MC-Dropout approximates epistemic uncertainty of DNNs that perform a regression, such as our SDC models [38], [42].

For the implementation of SDC models that support MC-Dropout, we followed the guidelines provided by Michelmore et al. [37]. The dropout layers are enabled at both training and testing time (in Keras, this is realized by setting `training=True` in the Dropout layers). With dropout enabled at testing time, predictions are no longer deterministic: given the same driving image, the model could predict slightly different steering angle values every time the image is processed by the DNN. All such predictions are interpreted as a probability distribution and the value predicted by the DNN is the expected value (mean) of such probability distribution, whereas the variance of the observed probability distribution quantifies the uncertainty. A higher variance marks lower confidence, whereas a lower variance indicates higher confidence [41].

In our *virtual* platform, we set the number of stochastic forward passes (i.e., the size of the sample used to estimate uncertainty) to match the batch size used during training (i.e., 64), whereas for the *physical* Donkey Car, we used a batch size of 16 which allows processing at  $\approx 20$  Hz on a limited GPU memory (even smaller values, such as 10, are deemed reasonable [41]).

## 5 EMPIRICAL STUDY

The *goal* of the empirical evaluation is compare the driving behaviour and failure exposure of virtual vs physical SDCs across digital and real-world test environments.

### 5.1 Research Questions

We consider the following research questions:

**RQ<sub>0</sub> (visual odometry accuracy):** *How accurate is visual odometry in estimating lateral position for autonomous vehicles driving in the real world?*

In RQ<sub>0</sub> we compare the accuracy of lateral position estimations made by visual odometry with human-defined

ground truth. The aim is to investigate whether this technique is accurate enough in the prediction of the lateral position metric on real-world data. This question serves as a prerequisite for our empirical study and will assess whether the lateral position predictions by the visual odometry can be reliably used as visual surrogates of the true odometry in the real world.

**RQ<sub>1</sub> (transferability of behaviour):** *Do the behavioral and quality metric distributions observed in simulation transfer to the metric distributions estimated by visual odometry or measured in the real environment?*

In this RQ we compare the driving profiles observed in the virtual vs physical world. Ideally, good and faithful virtual environments should reproduce the same profiles that would be experienced in the real world.

**RQ<sub>2</sub> (transferability of failures):** *What is the relation between system-level failures occurring in simulation and those observable in the real world? Can we expose the same real-world failures by running only the subset of tests that exhibit high telemetry (e.g., uncertainty) in the simulation?*

In this RQ we first compare the failures experienced during virtual vs physical system-level testing due to corrupted or adversarial settings. Ideally, good and faithful virtual environments should produce failures analogous to those experienced in the real world. Second, we consider whether developers could avoid expensive real-world executions whose non-failing behavior can be predicted by looking at simulation telemetry data (i.e., steering angle, XTE, or uncertainty), focusing the testing budget on more promising test scenarios, i.e., those exhibiting high telemetry in simulation.

## 5.2 Test Objects and Environment

### 5.2.1 Self Driving Car Models

We test three existing DNN-based SDCs: Nvidia’s DAVE-2 [26], Chauffeur [27], and Epoch [28]. We selected these models because they are robust, publicly available SDC models that have been objects of study in several testing works [5], [6], [7], [10], [11].

DAVE-2 consists of three convolutional layers, followed by five fully-connected layers. Chauffeur uses a convolutional neural network to extract the features of input images, and a recurrent neural network to predict the steering angle from 100 previous consecutively extracted features. Epoch is implemented as a simple convolutional neural network with three convolutional layers.

### 5.2.2 Camera Calibration

We matched all the parameters of the virtual camera in the simulator to those of the camera on the Donkey Car (a Sony 8MP IMX219). Specifically, we set 160 degrees of field-of-view (FOV), an aperture of 2.35 (F), a focal length of 3.15mm, and a sensor size of 16mm. Finally, we set the frame rate in the simulator the same as in the physical camera (i.e., 21 fps), and we positioned the simulated camera to match the height of the real-world camera so that images are captured under the same perspective.

For throttling, we set a constant throttle value of 0.2 in the simulator, corresponding to `THROTTLE_FORWARD_PWM = 500` in the physical car, resulting in a maximum driving speed of 3.1 mph (5 km/h, or 1.40 m/s).

### 5.2.3 Testing Tracks

We execute our experiments on the “DIYRobocars Standard Track” [43], 11m long track which is 52 cm wide. Clockwise, the track features three curves on the right and one on the left. For the simulator, we developed a new Unity scene that resembles the real-world room and track. To perform this task, we imported a high-resolution picture of the real track into Unity. This ensures that the track used in the simulator is identical in road shape and colors to the one in the real world and that the proportions of the car with respect to the track are maintained.

## 5.3 RQ<sub>0</sub>: Procedure and Metrics

### 5.3.1 CycleGAN Data Collection, Setup, and Training

We trained a CycleGAN model on 5,360 virtual images and 5,360 unpaired real-world images (the chosen GAN architecture does not need paired images), using the default hyper-parameters of the original paper [40]. Training images were collected with an original size of  $320 \times 240$  pixels, cropped to size  $320 \times 120$  to remove background noise, and reshaped to  $256 \times 256$  pixels, which is the default for CycleGAN. The output of the CycleGAN model is a new  $256 \times 256$  pixels image.

The network was trained for 75 epochs with the default learning rate of 0.0002, and for further 20 epochs featuring a linear decay of the learning rate towards zero. We visually assessed that the generated pseudo-real images highly resemble the real-world images. A detailed qualitative and quantitative evaluation of the outputs of generative networks is a challenging task with no consolidated solution [44], and out of the scope of this paper. We rather evaluate the output of CycleGAN in an operative way, i.e., by using its outputs to train an XTE predictor and testing its accuracy on real-world data. The effectiveness of the XTE predictor would also implicitly validate the images translated by CycleGAN in their ability to retain all essential features needed for an accurate prediction.

### 5.3.2 XTE Predictor Data Collection, Setup, and Training

Training data were collected by instrumenting the *virtual* DonkeyCar to drive for five laps in the simulator, following five different track trajectories along the track that would correspond to  $XTE = [-2, -1, 0, +1, +2]$ .

Overall, we obtained a balanced dataset of 5,362 training *virtual* images labeled with accurate XTE values that we translated to the corresponding *pseudo-real images* using CycleGAN. Such pseudo-real images produced by CycleGAN are labeled with XTE values obtained from the simulator for the corresponding simulated images (i.e., the CycleGAN’s input). This means that labeled training data can be produced automatically, with no human input. Then, we trained the XTE predictor setting the maximum number of epochs to 100, with a learning rate of 0.0001. The network uses the Adam optimizer to minimize the mean squared error (MSE) between the predicted XTE value and the ground truth value.

### 5.3.3 Metrics for visual odometry evaluation

For the purpose of answering RQ<sub>0</sub>, we collected additional test data by manually driving the *physical* DonkeyCar on

the real-world track and by labeling manually the collected frames with ground truth XTE values. In fact, with RQ<sub>0</sub> we want to evaluate the accuracy of the XTE predictor when deployed on the real SDC, where the input is a real-world image. To simplify frame capture, the speed was set to 0 mph and the car was moved from one position to the next manually. This was achieved by assigning the throttle’s PWM a value below a certain configurable value (`THROTTLE_FORWARD_PWM < 480` in our setting). With this setting, the vehicle is regarded as “active”, hence camera frame recording is enabled, even though the vehicle is not actually moving because the pulse width signal is too low to allow motion. This way we could capture frames of interest at different trajectories in a controllable way, by manually placing the vehicle at different locations on the track corresponding to the same five different trajectories of interest ( $XTE = [-2, -1, 0, +1, +2]$ , the same values considered during the training set data collection).

Overall, we obtained a dataset of 6,638 testing images, uniformly distributed over the five XTE classes. During testing, we evaluate the *accuracy* of the XTE predictor by measuring the mean absolute error (MAE) both numerically and in centimeters on the manually-labeled test set of real-world images.

## 5.4 RQ<sub>1</sub>: Procedure and Metrics

### 5.4.1 SDC Data Collection

To obtain two comparable datasets of driving data, for each testing environment (virtual and physical world), we collected a training set of 30 laps by manually driving on both the virtual and physical tracks with a joystick. We incentivize the car to stay close to the centerline of the track.

### 5.4.2 SDC Model Setup & Training

For each DNN (DAVE-2, Chauffeur, Epoch), we trained an individual SDC model on each training set (virtual and real-world), for a total of six models. The number of epochs was set to 500, with a batch size of 64 and a learning rate of 0.0001. We used early stopping with a patience of 30 and a minimum loss change of 0.0005 on the validation set. The DNNs use the Adam optimizer to minimize the MSE between the predicted steering angles and the ground truth value. We cropped the images to  $140 \times 320$  by removing 100 pixels from the top, and used data augmentation to mitigate the lack of image diversity in the training data using different image transformation techniques (e.g., translation, shadowing, brightness).

After training, we assessed that the six trained DNNs were able to drive in their corresponding testing tracks. We let each model drive for 50 consecutive laps and observed that they are able to drive without crashing or driving off-road ( $|XTE| < 2.22$  for all driving images). For the physical vehicle, we also carefully controlled the discharge of the Donkey Car’s battery and we recharged the battery if the voltage fell below 11.8V (12.7V being the maximum). Lower values were found to jeopardize the predictions and the quality of driving.

Prior to drawing conclusions across virtual and real-world models, we assessed whether the amount of available

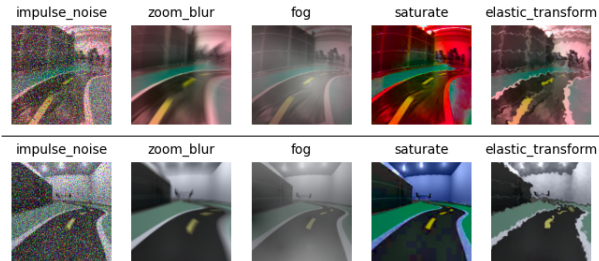


Fig. 1: Corruptions on real-world/virtual driving images

telemetry data was sufficient to characterize reliably each individual model. Specifically, we split the available telemetry data into two sets, one containing the driving data of the first 25 laps, and the second containing the driving data of the next 25 laps. Statistical power of the F-test for one factor ANOVA [45] was always above the conventional threshold  $\beta = 0.8$  and the  $p$ -value of the Mann-Whitney U test [46] was also above the conventional threshold  $\alpha = 0.05$ . This means that the telemetry data from the first 25 laps are statistically indistinguishable from those of the second 25 laps, both in the simulation and in the real environment. Thus, we can reliably use the metrics collected on such 50 laps for RQ<sub>1</sub>, i.e., transferability across environments.

### 5.4.3 Metrics for SDC Model Evaluation

We assess *transferability* of the quality of driving by analyzing the distributions of three metrics, namely *steering angle*, *lateral deviation*, and *predictive uncertainty* described in detail in Section 4. Both steering angle and XTE profiles characterize the behaviors of SDCs as erroneous steering angle predictions are likely to produce high positive or negative XTE values [10]. Uncertainty profiles do also characterize the driving behaviors from the point of view of the confidence (or lack thereof) of the DNN model while driving. We compare the distributions of these three metrics in the virtual vs physical track, to investigate the transferability of the observed driving behaviors between the two environments. Ideally, all three metrics should have similar distributions in the simulation and in the real world.

## 5.5 RQ<sub>2</sub>: Procedure and Metrics

### 5.5.1 Test Scenarios

As our SDC models are constructed to be failure-free in nominal conditions (RQ<sub>2</sub>), with RQ<sub>2</sub> we test them by injecting unknown conditions (i.e., conditions different from those in the training set) onto the existing tracks *in real-time during driving*. The main requirement is that such conditions should be applicable to virtual and physical settings alike. We chose two different kinds of image perturbations, one black-box, and one white-box.

Concerning the former, we test our SDCs under the image *corruptions* by Hendrycks et al. [47], commonly used to test DNNs that process imagery data. The paper proposes 19 corruptions belonging to five classes, namely *noise* (four types: gaussian, shot, impulse, speckle), *blur* (five types: gaussian, glass, defocus, motion, zoom), *weather* (four types: fog, frost, snow, rain), *luminance* (three types: contrast, brightness, saturate), and *resolution reduction* (three types:



Fig. 2: UAPr causing an OOT failure

JPEG compression, pixelate, elastic transform). Each corruption has a severity level from 1 to 5, indicating intensifying perturbations. Figure 1 shows a few examples of simulated and real-world driving images.

For what concerns the white-box perturbations, we test our models against *adversarial examples*. Unlike the corruptions by Hendrycks et al. [47], adversarial examples are minimal, synthetically crafted perturbations that cause a DNN to misbehave. In this paper we use the Universal Adversarial Perturbation on Regression (UAPr), a white-box targeted attack against end-to-end autonomous driving systems proposed by Wu and Ruan [48]. UAPr applies a universal perturbation to all driving frames of an autonomous vehicle, forcing it to drive in the desired direction (either left or right). This attack requires data-box access [29] because the adversarial image is learned offline using the images of the training set of the DNN under test. The universal perturbation is generated through training by linearizing the output of the DNN until the minimum perturbation that changes the sign of the prediction to the desired direction (i.e., either steering left, or steering right) is found. During real-time execution, adversarial examples are generated by applying the generated universal perturbation to each input image by summation (see Figure 2). We applied UAPr with two severity levels, either by adding the adversarial image as is or by doubling the magnitude of the perturbation it introduces. Moreover, we activated UAPr in the whole image stream starting from the beginning of the simulation (both for left and right), or only in the proximity of a curve (our testing track contains one left curve and three right curves), for a total of six configurations. Overall, we executed 642 one-lap simulations: 570 simulations enabling the corruptions (3 SDC models  $\times$  19 corruptions  $\times$  5 levels of severity  $\times$  2 testing environments) and 72 simulations enabling UAPr (3 SDC models  $\times$  6 configurations  $\times$  2 levels of severity  $\times$  2 testing environments).

Upon collecting failure results, we also aim to investigate whether we can reduce the number of real-world test scenarios based on the telemetry data measured on the corresponding scenarios in the virtual platform. In principle, all test configurations that fail in the simulator (if any) should be also executed in the real world. Differently, among the test configurations that are successful in the simulation, we may want to execute only those that exhibit high telemetry (e.g., uncertainty) in simulation. The main hypothesis is that for such configurations it might be possible to set a telemetry threshold to determine the trade-off between the number of configurations that can be potentially avoided (having low telemetry values) vs the number of failures missed if any.

### 5.5.2 Metrics

For each simulation, we classify its outcome using the following categorical scale: (1) *Successful (Succ.)* if the vehicle was able to travel the entirety of the track with no

TABLE 1: RQ<sub>0</sub>: Errors in XTE prediction by visual odometry

	MAE		
	#	cm	road width (%)
Outer lane (class 2)	0.26	2.98	5
Left lane (class 1)	0.14	1.58	3
Road center (class 0)	0.22	2.56	4
Right lane (class -1)	0.18	2.07	4
Inner lane (class -2)	0.21	2.49	4
Average	0.20	2.34	4

failures, (2) *OBE* (out-of-bound) failure, if the vehicle drove occasionally off-road while being able to recover back to the track and to complete the track, and (3) *OOT* (out-of-track) failure, if the vehicle drove off-road and was unable to recover back to the track. Clearly, OOT indicates a severe failure of the SDC, whereas OBE indicates a lower deviation from the main requirements.

Moreover, we divided our tracks into five distinct sectors and quantify the *Severity* of a failure. Indeed, driving off-road at some initial part of the track indicates a worse driving capability than driving off-road near the end of the track. We calculate the severity of a failure as:

$$Severity = \begin{cases} 0, & \text{if Succ.} \\ 1 + (5 - TrackSector), & \text{if OBE} \\ 10 + (5 - TrackSector), & \text{if OOT} \end{cases}$$

where *TrackSector* is an integer in the range 0–4. Thus, the *Severity* metric ranges from 0 (i.e., no failure, the simulation is successful) to 15 (i.e., the worst case of failure, with an OOT in the first sector).

To analyze whether we can reduce the number of real-world tests to be executed, we collect driving telemetry data (steering angle, XTE, and uncertainty) under corrupted/adversarial settings. Then, we consider the following cases: (1) executions that are successful both in simulated and real environments (Succ. Sim  $\rightsquigarrow$  Succ. Real), (2) executions that are successful in simulation but expose OBE failures in the real environment (Succ. Sim  $\rightsquigarrow$  OBE Real), and (3) executions that are successful in simulation but expose OOT failures in the real environment (Succ. Sim  $\rightsquigarrow$  OOT Real). We adopted a threshold corresponding to the median (50<sup>th</sup> percentile) of the driving data distribution for all virtual driving executions. Only test scenarios having steering/XTE/uncertainty values above the threshold are selected for real-world execution.

For the selected test cases, we count the true positives (TP: selected tests that fail in the real environment with OBE or OOT), the false positives (FP: selected tests that do not fail in the real environment), the true negatives (TN: discarded that do not fail in the real environment), and the false negatives (FN: discarded that fail in the real environment with OBE or OOT). Ideally, good test selection should achieve high TP, TN, and low FP, FN values. We also measure the estimated saving as the fraction of non executed test cases:  $Saving = (TN + FN) / (TP + TN + FP + FN)$ .

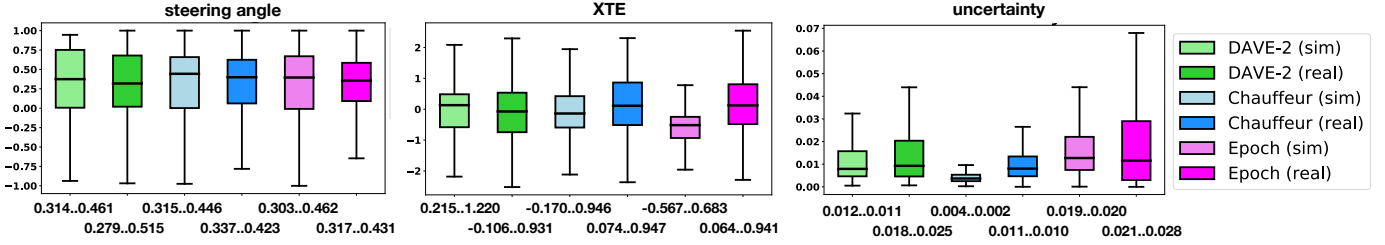


Fig. 3: RQ<sub>1</sub>: distributions of telemetry data and uncertainties in virtual vs physical test environments; x-axis: mean..stdev.

## 5.6 Results

### 5.6.1 Visual Odometry Accuracy (RQ<sub>0</sub>)

**Table 1** presents the accuracy results for visual odometry. Columns 2-3 report MAE values both numerically and in centimeters, whereas Column 4 reports the MAE error as a percentage of the track width. The table reports the results on a per-class basis and the average across classes. Overall, visual odometry yields good results. The most interpretable results are those in centimeters, with an average error of 2.34 cm, corresponding to only 4% of the road width.

[RQ<sub>0</sub>: The XTE estimation by visual odometry yields, on average, an error as small as 2.33 cm in the real-world, or 4% of the road width. We conclude that we can use visual odometry as a reliable technique to estimate the lateral position of real-world images to study transferability of SDC behaviour.]

### 5.6.2 Transferability of Behaviours (RQ<sub>1</sub>)

**Figure 3** compares the telemetry distributions for steering angle, XTE, and uncertainty for each SDC across environments. Statistical significance of the differences was assessed using the non-parametric Mann-Whitney U test [46] ( $\alpha = 0.05$ ), and the Cohen’s  $d$  effect size [45].

Concerning steering angle distributions, no statistically significant differences were found during virtual and physical simulations across all models ( $p$ -value  $> 0.05$ ; statistical power  $> 0.8$ ). This is not entirely surprising, as the SDC models under test share the same architecture, the number of parameters, and training hyperparameters, whereas they mainly differ for the datasets they are trained on (yet representing the same track). Therefore, it is somehow expected that the set of predictions to navigate the tracks in nominal conditions is comparable across environments and corroborates our efforts in trying to align the two testing environments (see [Section 5.2](#)).

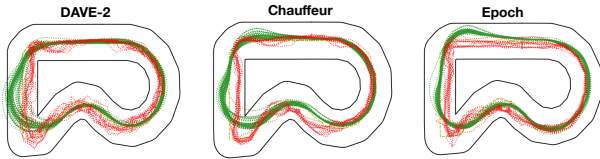


Fig. 4: Virtual (green) and physical (red) trajectories

Differently, XTE distributions are statistically different between virtual and physical simulations across all models ( $p$ -value  $< 0.05$ , with small/large/negligible effect sizes for DAVE-2/Chauffeur/Epoch). **Figure 3** shows the trajectories

of the SDCs. Trajectories by the physical Donkey Car (red) are less smooth than those of the simulated virtual self-driving car (green) as they are characterized by sharper angles and more frequent steering adjustments. This may be due to the intrinsically higher difficulty of driving in the real world as compared to the simulator: real-world images are noisier and more difficult to interpret automatically for the DNN. Other explanations for the distinctness have to do with the physical actuators involved in real-world driving and the latency between the DNN predictions and the reactions of the car’s mechanical components, which is absent in the simulator.

Our hypothesis is partially confirmed when looking at the model-level uncertainty distributions: we observed a statistically significant increase of the uncertainty values when predictions are made on the physical car ( $p$ -value  $< 0.05$ ; negligible/small/large effect sizes for DAVE-2/Chauffeur/Epoch). This means that the physical world introduces additional sources of uncertainty with respect to the simulated world due, for example, to ephemeral changes in illumination and noise, which may affect real images, while being absent in simulated images.

[RQ<sub>1</sub>: The steering angle distributions observed in simulation do transfer to a physical SDC equipped with the same model. Differently, XTE values do not transfer when considering a physical vehicle. Likewise, uncertainty estimation does not transfer and uncertainty values of a physical SDC are generally higher than those exhibited by a simulated SDC, possibly because of sources of non-stationarities, uncertainty, noise and mechanical latencies affecting real world driving.]

### 5.6.3 Transferability of Failures (RQ<sub>2</sub>)

**Table 2** presents the failures results separately for corruptions (aggregated by class) and adversarial examples. For each SDC model and for each testing environment, the table reports the number of configurations that are successful (Succ.), the number of those characterized by an OBE or by an OOT failure, and the severity score (Sever.).

Concerning image corruptions, DAVE-2 is the best performing SDC model with the least number of failures, both in simulated and physical environments. The blur effect is the most severe corruption as far as OBEs are concerned for 4 out of 6 SDC models. Regarding OOTs, the weather effect is consistently responsible for OOTs in the virtual environment, whereas the blur effect is the main source for OOTs in the physical environment. Overall, our results indicate an increasing number and severity of the failures

TABLE 2: RQ<sub>3</sub>: Failures of SDC models for virtual and physical test environments

	DAVE-2						Chauffeur						Epoch											
	sim			real			sim			real			sim			real								
	Succ.	OBE	OOT Sever.	Succ.	OBE	OOT Sever.	Succ.	OBE	OOT Sever.	Succ.	OBE	OOT Sever.	Succ.	OBE	OOT Sever.	Succ.	OBE	OOT Sever.	Succ.	OBE	OOT Sever.			
<b>Corruptions</b>																								
All	38	16	41	<b>6.0</b>	29	9	57	<b>8.2</b>	32	17	46	<b>6.9</b>	27	2	66	<b>8.9</b>	18	12	65	<b>9.2</b>	23	4	68	<b>9.4</b>
Noise	5	4	11	7.5	7	1	12	8.1	8	2	10	6.6	8	1	11	7.3	2	0	18	12.5	2	0	18	12.5
Blur	15	3	7	4.2	7	3	15	8.5	6	8	11	7.4	4	0	21	10.9	0	7	18	10.2	2	2	21	11.8
Weather	1	4	15	10.7	4	2	14	9.9	2	2	16	11.2	2	1	17	11.1	1	0	19	13.1	1	1	18	12.4
Luminance	7	2	6	5.4	1	1	13	11.2	6	2	7	7.0	1	0	14	12.6	5	2	8	7.9	5	1	9	8.5
Resolution Reduction	10	3	2	2.3	10	2	3	3.3	10	3	2	2.3	12	0	3	2.6	10	3	2	2.3	13	0	2	1.7
<b>Adversarial Examples</b>																								
All	0	0	12	<b>15.0</b>	0	0	12	<b>15.0</b>	4	4	4	<b>5.1</b>	12	0	0	<b>0.0</b>	0	0	12	<b>13.8</b>	2	0	10	<b>8.1</b>
No Steer Left	0	0	4	15.0	0	0	4	15.0	0	4	0	4.0	4	0	0	0.0	0	0	4	13.5	2	0	2	5.5
No Steer Right	0	0	8	15.0	0	0	8	15.0	4	0	4	6.3	8	0	0	0.0	0	0	8	14.0	0	0	8	10.8

TABLE 3: Failure matches across virtual and physical tests.

	DAVE-2		Chauffeur		Epoch		Total	
	#	%	#	%	#	%	#	%
<b>Corruptions</b>								
sim ✓ real ✓	49	17	48	17	68	24	165	58
sim ✗ real ✓	10	4	18	6	16	6	44	15
sim ✓ real ✗	36	13	29	10	11	4	76	27
<b>Adversarial Examples</b>								
sim ✓ real ✓	12	100	4	33	4	8	20	56
sim ✗ real ✓	0	0	8	67	8	4	16	44
sim ✓ real ✗	0	0	0	0	0	0	0	0

due to corruptions in the real environment (for Severity: +37% for DAVE-2, +29% for Chauffeur, and +2% for Epoch).

Concerning adversarial attacks, DAVE-2 is the worst model, being unable to complete any virtual or physical simulation, while Chauffeur proved very robust to UAPr in the physical environment, with no failures exhibited by the Donkey Car. The trend observed under adversarial attacks is opposite to the trend observed with corruptions: in the former case, the physical environment is more resilient to attacks than the simulator. The higher variability of real images, combined with the sources of noise in the real world, makes adversarial attacks less effective than on the clean, artificial images produced by the simulator, where pixel values are more predictable and hence more attackable.

In Table 3, for each individual configuration (285 overall for corruptions and 36 for adversarial examples), we report the number of times in which the severity score was the same across environments, in which the severity score was worse for the virtual than for the physical environment, and vice-versa on a per-model basis and in total. Overall, we found that nearly 60% of the configurations do generalize from simulated to real-world environments. For corruptions, the severity is usually amplified from virtual to physical environments, which means that we cannot completely avoid testing for corruptions in the physical environment. Differently, no adversarial attacks on real-world images were found worse than the corresponding virtual ones. This essentially means that we can reliably test SDC under adversarial attacks in simulation platforms only, with a good likelihood of the results being transferable to a physical SDC with the same DNN model.

Concerning real-world test reduction, we discarded the steering angle metric since values were found indistinguish-

TABLE 4: Test selection based on uncertainty for configurations above the median: true/false positives/negatives

	Succ. Sim $\rightsquigarrow$		Succ. Real		OBE Real		OOT Real		Tot. Sim.	Saving		
	FP	TN	TP	FN	TP	FN	TP	FN		#	#	%
DAVE-2	4	17	4	0	10	2	37	19	51	4.28		
Chauffeur	9	13	-	-	6	2	30	15	50	4.17		
Epoch	8	10	-	-	1	0	19	10	53	4.39		
Total	21	40	4	0	17	4	86	44	51	12.83		

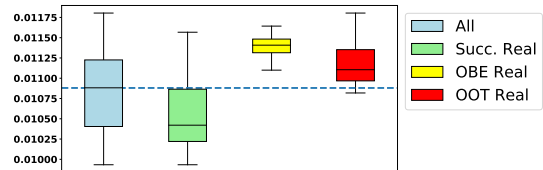


Fig. 5: For DAVE-2 all test configuration with average uncertainty above the median are not executed in the real-world.

able across environments (RQ<sub>1</sub>). For conciseness of presentation, we also discarded the XTE metric, as it was found ineffective for test selection. The only metric yielding promising results is predictive uncertainty. Table 4 shows the results concerning the real-world test reduction achievable through the analysis of SDCs' predictive uncertainty during the virtual simulations. For each SDC model, Table 4 reports the associated true/false positive/negative numbers, using the median as a threshold on the uncertainty values of all virtual simulations. Results show a high reduction rate: for 40/61 configurations (66%), physical testing on the Donkey Car can be safely avoided (TN Succ. Real). At the same time, all 4 OBE failures (100% of OBE Real) and a large fraction of OOTs (17/21, 81% of OOT Real) are exposed in the real world, and only 4 OOT failures are missed. The expected time saving is quite high as 44/86 (51%) configurations do not need further real-world testing. In our setting, this saving amounts to  $\approx 13$  hours, considering an average of 5 min/test case execution in the physical environment.

Figure 5 shows the uncertainty distributions for DAVE-2, the only SDC model characterized by high failure variance across environments (see Table 4). For DAVE-2, the median uncertainty threshold of 0.01088 provides a good cut-off value for the estimation of the real-world behavior.

⌈ **RQ<sub>2</sub>**: System-level failures triggered by corruptions of the input images are more frequent in the real world than in simulation and tend to have higher severity. This may indicate that the simulator ignores real-world details that are important to expose failures. Interestingly, the opposite happens under adversarial attacks, that are less successful in the real world than in simulation. Model uncertainty allows to prioritize the successful simulations for real-world execution, providing an estimated time saving of around 51%, countered by just 5% missed executions. ⌋

## 5.7 Threats to Validity

### 5.7.1 Internal validity

We compared all SDCs under identical parameter settings. One threat to internal validity concerns our custom implementation of the racing track within the simulator. However, this was unavoidable. We started from a picture of the real-world track to maintain its exact proportions and tried to reproduce the environment as faithfully as possible. Another threat may be due to our own data collection phase and training of SDCs, which may exhibit a large number of misbehaviors if trained inadequately or with poor quality data. We mitigated this threat by training and fine-tuning the best publicly available driving models, which were able to drive consistently in nominal conditions and were failing only in unseen conditions.

### 5.7.2 External validity

We used a limited number of SDC models in our evaluation, which poses a threat in terms of the generalizability of our results. We tried to mitigate this threat by choosing popular real-world SDC models which achieved competitive scores in the Udacity challenge. We considered only one physical track and only one 1/16 scale physical car. However, DonkeyCar was used as a proxy for full size SDCs also in previous studies [18], [22], [23], [24]. Other similar, small-scale platforms were found to retain key environmental characteristics experienced by full-scale SDCs [18].

### 5.7.3 Reproducibility

The software artifacts, our results, demo videos, and the simulator are available [49]. To replicate our study, however, two open-source physical assets are needed, i.e., a DonkeyCar and the racing track ( $\approx 500\$$ ).

## 6 DISCUSSION

### 6.1 Virtual vs Physical Testing

Simulators are unhitched from the limits of real-life and thus real-world driving maneuvers can be amplified into hundreds or more simulated scenarios to probe the edges of the vehicle’s capabilities [50]. Thus, simulators are advantageous as long as they are able to represent the real-world environment and the SDC’s sensors with high-fidelity. However, our results indicate that a gap exists between the testing results from *in-vitro* simulated experiments and the real-world *in-vivo* observations of deployed models. We hypothesize the main root causes being the poor photo-realism and the inadequate representation of the vehicle’s sensory and of the environmental uncertainty sources.

The virtual world available in the Donkey Car simulator offers a simplified representation of the complexity of the physical self-driving car platform as it omits subtle visual cues that are important for driving scene processing, and that can ultimately flummox the car. Moreover, in the physical car, driving is affected by inevitable real-time stochasticities that are immaterial in the virtual world. For instance, the throttle control can be adversely affected by the friction of the surface and battery voltage, whereas steering angle prediction can be affected by noise such as sudden spikes in luminosity, latency between prediction and actuation, and other forms of disturbances that are unveiled only in a physical setting.

Hence, given the current state of the practice, a certain degree of testing under physical conditions is still necessary to help identify and correctly handle discrepancies between the virtual and real environments. In our work, we tried to quantify such analogies and differences using a small-scale open-source EV vehicle. For a good number of conditions ( $\approx 60\%$ ), testing results do generalize across environments. This may be due to a faithful digital recreation of the real-world testing environment, necessary to fully exploit simulated testing, as suggested by industrial practices [2], [3], [4]. Differently, for the mismatching cases, we have shown that MC-Dropout uncertainty on the virtual platform allows the selection of the most promising test cases that need to be executed in the real world. The potential saving for our rather short track ( $-12.8$  hours) may be amplified substantially on longer tracks in which tests unlikely to expose failures in the real world represent a major cost.

### 6.2 Possible Applications of CycleGAN

The CycleGAN that we used for visual odometry could find applications that go beyond real-world metric estimation.

Previous work [8] comparing offline vs online testing suffers from the problem of aligning labeled data from the two environments (real and simulated world), as the offline training datasets of real-world driving images with steering angle labels (e.g., by Udacity’s [51] or Waymo’s [52]) might be difficult to pair with labeled simulated images obtained from a simulator. Such alignment was achieved heuristically [8]; with CycleGAN, developers and researchers could translate real images to pseudo-simulated ones, and then find the closest labeled image from the simulated dataset, according to some pixel-wise distance metric.

CycleGANs could be useful in the context of reinforcement learning-based autonomous driving [53], as the estimated XTE could provide the necessary reward signal during training. Indeed, our visual odometry approach could be utilized to estimate XTE more accurately than existing computer vision heuristics that are hard to tune [54].

Concerning the usage of real-world driving scenes to inform the driving in simulation, we envision two main applications. First, CycleGAN could be used for producing photo-realistic training data that could help the training of SDC in the simulator but with pseudo-real data gathered from on-road testing. Second, CycleGAN could be also useful to perform system-level virtual testing on pseudo-real testing environments that are dynamically generated and loaded at runtime as the simulated vehicle executes. In

addition to translating and replacing the output of the camera sensor, one could also devise a decoupled architecture in which a middleware layer abstracts the entire hardware sensory [55] and makes it available to the simulator through the translation performed by a CycleGAN.

## 7 RELATED WORK

### 7.1 Model- and System-level Testing Approaches

Most approaches use *model-level testing* to test DNN autopilots under corrupted images [5], [6] or GAN-generated driving scenarios [7] without however testing the self-driving software on its target environment. Dang et al. [56] study the robustness of DNN driving models with respect to different adversarial attacks. While we also use (universal) adversarial attacks, differently, in our work, we focus on system-level testing and on simulated vs real SDCs, finding simulated SDCs generally more susceptible to adversarial attacks than their real-world counterparts when tested at the system level. Concerning *system-level testing* techniques for AVs, researchers proposed techniques to generate scenarios that cause AVs to misbehave [11], [15], [42], [50], [57]. These works only consider simulated testing, whereas we compared virtual vs physical environments. The applicability of test generators to real driving scenarios remains unexplored.

### 7.2 Empirical Studies

Recent works have confirmed the need for real-world testing of robotic systems, as simulation platforms are often decoupled from the real world complexities [16], [17]. Our work is the first one to quantify such a reality gap and confirms the existing anecdotal knowledge in the field of autonomous driving.

Other works investigate the relation between model-level vs system-level testing metrics within a simulation environment. Codevilla et al. [9] found that offline prediction errors are not correlated with driving quality, and two DNN models with analogous error prediction rates may differ substantially in their driving quality. Haq et al. [8] compare the distributions of offline vs online predictions, but they consider only simulated environments (i.e., virtual SDCs) for the online predictions. They also compare offline and online errors, finding offline testing more “optimistic” than online simulation, as the accumulation of small, acceptable offline errors might result in safety online violations, during the simulation. In our empirical work, we focused on the difference between simulated and real-world environments, rather than offline vs online testing. We found a measurable gap between virtual and physical environments during system-level testing, which questions the transferability between simulation and real environment, a previously unexplored topic.

### 7.3 Virtual vs Physical Testing of Autonomous Vehicles

Chen et al. [58] embed a real hardware control unit within a simulation platform to verify the validity of self-driving DNNs in virtual scenes, including perception, planning, decision making, and control. Differently, we do not hybridize simulation and real-world testing, as our goal is to understand the transferability between the two.

Researchers have been using Donkey Car [22], [23], [24] or other frameworks [25], [53] to study reinforcement learning algorithms for autonomous driving. Verma et al. [18] compare different scaled vehicles concluding that such platforms allow the rapid exploration of many different test tracks while retaining realistic environmental conditions, which provides further justification for our choice to use Donkey Car.

### 7.4 GAN-based Testing of Autonomous Vehicles

Researchers tried to close the reality gap between the simulated vs real-world data by training Generative Adversarial Networks (GANs) to translate an input from one distribution to an input that resembles the characteristics of another distribution. DeepRoad [7] uses UNIT [59] to generate accurate photo-realistic paired driving scenes for SDC testing, which were evaluated for their capability of exposing individual prediction errors. Kong et al. [60] generate realistic adversarial billboards within real-world images that are able to confound the vehicle. In our work, we also use universal adversarial perturbation at the system level, finding comparable results in terms of virtual/physical robustness. SilGAN [61] uses GANs to generate driving maneuvers for software-in-the-loop testing. SurfelGAN [62] is a technique developed at Waymo to generate realistic sensor data for autonomous driving simulation without requiring manual creation of virtual environments and objects.

Differently from existing works, we use CycleGAN, which requires no pairing, to generate pseudo-real driving scenes that can inform a telemetry predictor to support virtual vs physical testing.

## 8 CONCLUSIONS

Virtual testing of autonomous vehicles with simulators is widely adopted. However, the lack of adequate fidelity and environmental modeling threatens the generalizability of testing results to the real world. While the development of scalable, physically accurate, and highly photo-realistic simulators is cornerstone for autonomous vehicle development, real-world testing with physical vehicles remains important, as our empirical study on a scaled vehicle shows that some DNN failures can be exposed only in real-world conditions.

Our empirical results also indicate that visual odometry can be used to obtain accurate telemetry data from real SDCs, making the physical environment comparably data-rich and informative as the simulated environment. We found that the quality of driving metrics like XTE tends to be worse when collected from a real SDC, probably due to the sources of noise (e.g., illumination changes) and to the stochastic effects of mechanical components (e.g., mechanical latency, friction), which are difficult to simulate accurately in the virtual environment. We also found a practical way to reduce the cost of real-world testing, based on uncertainty measures taken in simulation: successful test scenarios should be prioritized by decreasing uncertainty when scheduling them for execution on a real SDC.

In our future work, we will further investigate the failure conditions, root causes, and failure types associated with the reality gap between physical and virtual testing environments for autonomous driving systems.

## ACKNOWLEDGMENTS

This work was partially supported by the H2020 project PRECRIME, funded under the ERC Advanced Grant 2017 Program (ERC Grant Agreement n. 787703). We thank Roberto Minelli for the engineering advice and support concerning the DonkeyCar.

## REFERENCES

- [1] V. G. Cerf, "A Comprehensive Self-driving Car Test," *Commun. ACM*, vol. 61, pp. 7–7, Jan. 2018.
- [2] BGR Media, LLC, "Waymo's self-driving cars hit 10 million miles." <https://techcrunch.com/2018/10/10/waymos-self-driving-cars-hit-10-million-miles>, 2018. Online.
- [3] "Waymo Driver." <https://waymo.com/waymo-driver/>, 2021.
- [4] "Waymo Secret Testing." <https://www.theatlantic.com/technology/archive/2017/08/inside-waymos-secret-testing-and-simulation-facilities/537648/>, 2017.
- [5] K. Pei, Y. Cao, J. Yang, and S. Jana, "DeepXplore: Automated Whitebox Testing of Deep Learning Systems," in *Proceedings of the 26th Symposium on Operating Systems Principles, SOSP '17*, (New York, NY, USA), pp. 1–18, ACM, 2017.
- [6] Y. Tian, K. Pei, S. Jana, and B. Ray, "DeepTest: Automated Testing of Deep-neural-network-driven Autonomous Cars," in *Proceedings of the 40th International Conference on Software Engineering, ICSE '18*, (New York, NY, USA), pp. 303–314, ACM, 2018.
- [7] M. Zhang, Y. Zhang, L. Zhang, C. Liu, and S. Khurshid, "Deep-Road: GAN-based Metamorphic Testing and Input Validation Framework for Autonomous Driving Systems," in *Proceedings of the 33rd ACM/IEEE International Conference on Automated Software Engineering, ASE 2018*, (USA), pp. 132–142, ACM, 2018.
- [8] F. U. Haq, D. Shin, S. Nejati, and L. Briand, "Comparing Offline and Online Testing of Deep Neural Networks: An Autonomous Car Case Study," in *Proceedings of 13th IEEE International Conference on Software Testing, Verification and Validation, ICST '20*, IEEE, 2020.
- [9] F. Codevilla, A. M. López, V. Koltun, and A. Dosovitskiy, "On Offline Evaluation of Vision-based Driving Models," *CoRR*, vol. abs/1809.04843, 2018.
- [10] G. Jahangirova, A. Stocco, and P. Tonella, "Quality Metrics and Oracles for Autonomous Vehicles Testing," in *Proceedings of 14th IEEE International Conference on Software Testing, Verification and Validation, ICST '21*, IEEE, 2021.
- [11] A. Stocco, M. Weiss, M. Calzana, and P. Tonella, "Misbehaviour Prediction for Autonomous Driving Systems," in *Proceedings of 42nd International Conference on Software Engineering, ICSE '20*, ACM, 2020.
- [12] K. Yin, P. Arcaini, T. Yue, and S. Ali, "Analyzing the Impact of Product Configuration Variations on Advanced Driver Assistance Systems with Search," in *Proceedings of the Genetic and Evolutionary Computation Conference, GECCO '21*, (New York, NY, USA), p. 1106–1114, Association for Computing Machinery, 2021.
- [13] P. Arcaini, X.-Y. Zhang, and F. Ishikawa, "Targeting Patterns of Driving Characteristics in Testing Autonomous Driving Systems," in *2021 14th IEEE Conference on Software Testing, Verification and Validation (ICST)*, pp. 295–305, 2021.
- [14] T. Laurent, P. Arcaini, F. Ishikawa, and A. Ventresque, "Achieving Weight Coverage for an Autonomous Driving System with Search-based Test Generation," in *25th International Conference on Engineering of Complex Computer Systems (ICECCS)*, pp. 93–102, 2020.
- [15] A. Gambi, M. Mueller, and G. Fraser, "Automatically Testing Self-driving Cars with Search-based Procedural Content Generation," in *Proceedings of the 28th ACM SIGSOFT International Symposium on Software Testing and Analysis, ISSTA 2019*, (New York, NY, USA), pp. 318–328, ACM, 2019.
- [16] S. García, D. Strüber, D. Brugali, T. Berger, and P. Pelliccione, "Robotics Software Engineering: A Perspective from the Service Robotics Domain," in *Proceedings of the 28th ACM Joint Meeting on European Software Engineering Conference and Symposium on the Foundations of Software Engineering, ESEC/FSE 2020*, (USA), p. 593–604, Association for Computing Machinery, 2020.
- [17] A. Afzal, D. S. Katz, C. Le Goues, and C. S. Timperley, "Simulation for Robotics Test Automation: Developer Perspectives," in *2021 14th IEEE Conference on Software Testing, Verification and Validation (ICST)*, pp. 263–274, 2021.
- [18] A. Verma, S. Bagkar, N. V. S. Allam, A. Raman, M. Schmid, and V. N. Krovi, "Implementation and Validation of Behavior Cloning Using Scaled Vehicles," in *SAE WCX Digital Summit*, SAE International, apr 2021.
- [19] A. Bulsara, A. Raman, S. Kamarajugadda, M. Schmid, and V. N. Krovi, "Obstacle avoidance using model predictive control: An implementation and validation study using scaled vehicles," tech. rep., SAE Technical Paper, 2020.
- [20] "Donkey Car." <https://www.donkeycar.com/>, 2021.
- [21] "AWS DeepRacer." <https://aws.amazon.com/deepracer>, 2021.
- [22] H. Zhou, X. Chen, G. Zhang, and W. Zhou, "Deep Reinforcement Learning for Autonomous Driving by Transferring Visual Features," in *2020 25th International Conference on Pattern Recognition (ICPR)*, pp. 4436–4441, 2021.
- [23] A. Viitala, R. Boney, and J. Kannala, "Learning to Drive Small Scale Cars from Scratch," *CoRR*, vol. abs/2008.00715, 2020.
- [24] Q. Zhang and T. Du, "Self-driving scale car trained by Deep reinforcement Learning," *CoRR*, vol. abs/1909.03467, 2019.
- [25] B. Balaji, S. Mallya, S. Genc, S. Gupta, L. Dirac, V. Khare, G. Roy, T. Sun, Y. Tao, B. Townsend, E. Calleja, S. Muralidhara, and D. Karuppasamy, "DeepRacer: Educational Autonomous Racing Platform for Experimentation with Sim2Real Reinforcement Learning," *CoRR*, vol. abs/1911.01562, 2019.
- [26] M. Bojarski, D. D. Testa, D. Dworakowski, B. Firner, B. Flepp, P. Goyal, L. D. Jackel, M. Monfort, U. Muller, J. Zhang, X. Zhang, J. Zhao, and K. Zieba, "End to End Learning for Self-Driving Cars," *CoRR*, vol. abs/1604.07316, 2016.
- [27] Team Chauffeur, "Steering angle model: Chauffeur." <https://github.com/udacity/self-driving-car/tree/master/steering-models/community-models/chauffeur>, 2016. Online.
- [28] Team Epoch, "Steering angle model: Epoch." <https://github.com/udacity/self-driving-car/tree/master/steering-models/community-models/cg23>, 2016. Online.
- [29] V. Riccio, G. Jahangirova, A. Stocco, N. Humbatova, M. Weiss, and P. Tonella, "Testing Machine Learning based Systems: A Systematic Mapping," *Empirical Software Engineering*, 2020.
- [30] N. Humbatova, G. Jahangirova, G. Bavota, V. Riccio, A. Stocco, and P. Tonella, "Taxonomy of Real Faults in Deep Learning Systems," *ICSE'20*, (New York, NY, USA), ACM, 2020.
- [31] A. Dosovitskiy, G. Ros, F. Codevilla, A. López, and V. Koltun, "CARLA: An Open Urban Driving Simulator," *CoRR*, vol. abs/1711.03938, 2017.
- [32] "DeepDrive Voyage." <https://deepdrive.voyage.auto/leaderboard/>, 2019.
- [33] M. G. Bechtel, E. McEllhiney, M. Kim, and H. Yun, "DeepPicar: A Low-cost Deep Neural Network-based Autonomous Car," 2018.
- [34] "Robocar Store." <https://github.com/NVIDIA-AI-IOT/jetracer>, 2021.
- [35] F. Chollet et al., "Keras." <https://keras.io>, 2015.
- [36] "Unity3D." <https://unity.com>, 2019.
- [37] R. Michelmore, M. Wicker, L. Laurenti, L. Cardelli, Y. Gal, and M. Kwiatkowska, "Uncertainty Quantification with Statistical Guarantees in End-to-End Autonomous Driving Control," in *2020 IEEE International Conference on Robotics and Automation, ICRA 2020*, pp. 7344–7350, IEEE, 2020.
- [38] A. Stocco and P. Tonella, "Towards Anomaly Detectors that Learn Continuously," in *Proceedings of ISSREW 2020*, IEEE, 2020.
- [39] D. Scaramuzza and F. Fraundorfer, "Visual Odometry [Tutorial]," *IEEE Robotics Automation Magazine*, vol. 18, no. 4, pp. 80–92, 2011.
- [40] J. Zhu, T. Park, P. Isola, and A. A. Efros, "Unpaired Image-to-Image Translation using Cycle-Consistent Adversarial Networks," *CoRR*, vol. abs/1703.10593, 2017.
- [41] Y. Gal and Z. Ghahramani, "Dropout as a Bayesian Approximation: Representing Model Uncertainty in Deep Learning," in *Proceedings of the 33rd International Conference on International Conference on Machine Learning - Volume 48, ICML '16*, JMLR.org, 2016.
- [42] A. Stocco and P. Tonella, "Confidence-driven Weighted Retraining for Predicting Safety-Critical Failures in Autonomous Driving Systems," *Journal of Software: Evolution and Process*, 2021.
- [43] "DIYRobocars Standard Track." <https://www.robocarstore.com/collections/tracks/products/diyrobocars-standard-track>, 2021.
- [44] A. Borji, "Pros and Cons of GAN Evaluation Measures," *CoRR*, vol. abs/1802.03446, 2018.
- [45] J. Cohen, *Statistical power analysis for the behavioral sciences*. Hillsdale, N.J.: L. Erlbaum Associates, 1988.
- [46] F. Wilcoxon, "Individual Comparisons by Ranking Methods," *Biometrics Bulletin*, vol. 1, p. 80, Dec. 1945.

- [47] D. Hendrycks and T. G. Dietterich, "Benchmarking Neural Network Robustness to Common Corruptions and Perturbations," *CoRR*, vol. abs/1903.12261, 2019.
- [48] H. Wu and W. Ruan, "Adversarial Driving: Attacking End-to-End Autonomous Driving Systems," *CoRR*, vol. abs/2103.09151, 2021.
- [49] "Replication package." <https://github.com/tsigalko18/transferability-testing-sdcs>, 2021.
- [50] V. Riccio and P. Tonella, "Model-Based Exploration of the Frontier of Behaviours for Deep Learning System Testing," in *Proceedings of ACM Joint European Software Engineering Conference and Symposium on the Foundations of Software Engineering*, ESEC/FSE '20, 2020.
- [51] Udacity, "Self-driving car's datasets." <https://github.com/udacity/self-driving-car/tree/master/datasets>, 2017. Online.
- [52] Waymo LLC, "Waymo Open Dataset." <https://waymo.com/open/>, 2021. Online.
- [53] M. O'Kelly, H. Zheng, D. Karthik, and R. Mangharam, "Fltenth: An open-source evaluation environment for continuous control and reinforcement learning," in *Proceedings of the NeurIPS 2019 Competition and Demonstration Track* (H. J. Escalante and R. Hadsell, eds.), vol. 123 of *Proceedings of Machine Learning Research*, pp. 77–89, PMLR, 08–14 Dec 2020.
- [54] B. R. Kiran, I. Sobh, V. Talpaert, P. Mannion, A. A. A. Sallab, S. Yogamani, and P. Pérez, "Deep Reinforcement Learning for Autonomous Driving: A Survey," 2021.
- [55] C. Hildebrandt and S. Elbaum, "World-in-the-loop simulation for autonomous systems validation," in *2021 IEEE International Conference on Robotics and Automation (ICRA)*, 2021.
- [56] Y. Deng, X. Zheng, T. Zhang, C. Chen, G. Lou, and M. Kim, "An Analysis of Adversarial Attacks and Defenses on Autonomous Driving Models," 2020.
- [57] G. E. Mullins, P. G. Stankiewicz, R. C. Hawthorne, and S. K. Gupta, "Adaptive generation of challenging scenarios for testing and evaluation of autonomous vehicles," *Journal of Systems and Software*, vol. 137, pp. 197–215, 2018.
- [58] S. Chen, Y. Chen, S. Zhang, and N. Zheng, "A Novel Integrated Simulation and Testing Platform for Self-Driving Cars With Hardware in the Loop," *IEEE Transactions on Intelligent Vehicles*, vol. 4, no. 3, pp. 425–436, 2019.
- [59] M. Liu, T. M. Breuel, and J. Kautz, "Unsupervised Image-to-Image Translation Networks," *CoRR*, vol. abs/1703.00848, 2017.
- [60] Z. Kong and C. Liu, "Generating Adversarial Fragments with Adversarial Networks for Physical-world Implementation," *CoRR*, vol. abs/1907.04449, 2019.
- [61] D. Parthasarathy and A. Johansson, "SilGAN: Generating driving maneuvers for scenario-based software-in-the-loop testing," *CoRR*, vol. abs/2107.07364, 2021.
- [62] Z. Yang, Y. Chai, D. Anguelov, Y. Zhou, P. Sun, D. Erhan, S. Rafferty, and H. Kretschmar, "SurfelGAN: Synthesizing Realistic Sensor Data for Autonomous Driving," *CoRR*, vol. abs/2005.03844, 2020.